Journal of Dental Research
2022, Vol. 101(1) 73–82

DOI: 10.1177/00220345211013722
journals.sagepub.com/home/jdr

# Alveolar Bone Marrow Gli1$^+$ Stem Cells Support Implant Osseointegration

**Y. Yi[1,2,3], W. Stenberg[2], W. Luo[2], J.Q. Feng[2], and H. Zhao[1]**

**Abstract**

Osseointegration is the key issue for implant success. The in vivo properties of cell populations driving the osseointegration process have remained largely unknown. In the current study, using tissue clearing–based 3-dimensional imaging and transgenic mouse model-based lineage tracing methods, we identified Gli1+ cells within alveolar bone marrow and their progeny as the cell population participating in extraction socket healing and implant osseointegration. These Gli1$^+$ cells are surrounding blood vessels and do not express lineage differentiation markers. After tooth extraction and delayed placement of a dental implant, Gli1$^+$ cells were activated into proliferation, and their descendants contributed significantly to new bone formation. Ablation of Gli1$^+$ cells severely compromised the healing and osseointegration processes. Blockage of canonical Wnt signaling resulted in impaired recruitment of Gli1$^+$ cells and compromised bone healing surrounding implants. Collectively, these findings demonstrate that Gli1$^+$ cells surrounding alveolar bone marrow vasculature are stem cells supporting dental implant osseointegration. Canonical Wnt signal plays critical roles in regulating Gli1$^+$ stem cells.

**Keywords:** periodontium, hedgehogs, Wnt signaling pathway, bone-implant interface, dental implantation, alveolar bone

## Introduction

Since the introduction of the concept of "osseointegration" in 1969 (Branemark et al. 1969), implant treatment has gradually become a standard treatment for tooth loss (Buser et al. 2017). Among all the treatment options, delayed implant is a classical approach offering long-term stability and low failure risk (Canellas et al. 2019). However, there are still many challenges that hinder the success rate, such as reduction in bone dimensions after tooth extraction (Chappuis et al. 2013) and insufficient new bone formation around implants. As drivers of osteogenesis, resident stem cells in alveolar bone are thought to be recruited to the injury site and contribute to the pool of osteoblasts forming bone at extraction sockets and around implants (Tuan 2011; Zhang, Li, et al. 2020). Although some previous studies have shown the presence of osteogenic progenitor cells in the periodontal ligament (PDL) and their contribution toward osseointegration (Pei et al. 2017; Yuan, Pei, Zhao, Li, et al. 2018), their in vivo properties remain largely unknown.

The lack of in vivo studies on stem cell sources for dental implant osseointegration is partially due to the technical challenge for studying the intact implant–tissue interface. Histological sectioning, which requires removal of implants, inevitably destroys the integrity of the implant–tissue interface (He et al. 2017). Ground sectioning quenches endogenous fluorescence and generates very few sections (Calvo-Guirado et al. 2010), limiting its application on lineage tracing studies with transgenic reporter mice. Tissue clearing is a powerful tool for 3-dimensional (3-D) imaging. It turns tissues transparent by removing components blocking or diffracting the light inside the tissue (Tainaka et al. 2016). Recently, our lab developed the polyethylene glycol–associated solvent system (PEGASOS), which could clear hard and soft tissues without losing endogenous fluorescence (Jing et al. 2018, 2019). We introduced this technique to investigate the vasculature at the implant–bone interface (Yi et al. 2019).

Gli1$^+$ cells have been recognized as stem cells in many tissues (Schneider et al. 2017; Sena et al. 2017; Shi et al. 2017), especially in the craniofacial region (Zhao et al. 2014, 2015; Men et al. 2020). Recently, our group identified Gli1$^+$ cells within the adult mouse periodontal ligament as stem cells supporting periodontal tissue turnover and injury repair (Men et al. 2020). In addition to PDL, a few Gli1$^+$ cells were also detected within the alveolar bone marrow.

In this study, using a tissue clearing–based 3-D imaging method, we investigated the properties of Gli1$^+$ cells within the alveolar bone marrow before and after the titanium implant

[1]Department of Comprehensive Dentistry, College of Dentistry, Texas A&M University, Dallas, TX, USA
[2]Department of Biomedical Sciences, College of Dentistry, Texas A&M University, Dallas, TX, USA
[3]State Key Laboratory of Oral Diseases, West China School of Stomatology, Sichuan University, Chengdu, China

A supplemental appendix to this article is available online.

**Corresponding Author:**
H. Zhao, Department of Comprehensive Dentistry, College of Dentistry, Texas A&M University, Dallas, TX 75246, USA.
Email: huzhaolab@gmail.com

placement. With lineage tracing, we showed that Gli1$^+$ cells in alveolar bone marrow respond to tooth extraction, proliferate along blood vessels, and contribute to socket healing and implant osseointegration. Canonical Wnt signaling pathway plays a critical role in this process.

## Materials and Methods

### Animals

The Institutional Animal Care and Use Committee at Texas A&M University reviewed and approved all protocols for animal care and experiments. This study conformed with the ARRIVE guidelines for preclinical studies. *Gli1-Cre$^{ERT2}$* mice (JAX#007913), *Ai14* tdTomato reporter mice (JAX#007908), and β-*Catenin$^{flox/flox}$* (JAX#004152) and *ROSA26$^{eGFP\text{-}DTA}$* (JAX#006331) mice were purchased from the Jackson Laboratories. *Cdh5-Cre$^{ERT2}$* mice (Eilken et al. 2017) were provided by Dr. Woo-Ping Ge at the University of Texas Southwestern Medical Center for blood vessel investigation. To induce Cre activity, tamoxifen (Sigma Prod. No. T5648; Sigma Aldrich) dissolved in corn oil (20 mg/mL) was injected intraperitoneally (1.5 mg/10 g body weight) daily for 2 consecutive days.

### Tooth Extraction and Delayed Implant Placement Surgeries

Six-week-old mice were used for mandibular tooth extraction procedure. Tamoxifen was injected 5 d prior to the surgery for 2 consecutive days. Three mandibular molars were removed under anesthesia. Sockets were cleaned with a low-speed hand drill to remove the remaining PDL.

For delayed implant placement experiments, mandibular first molars were extracted at 3 wk of age. Tamoxifen was injected 3 wk after extraction. On day 25 after extraction, a 0.5-mm osteotomy was created in the healed extraction site with a low-speed hand drill. A titanium implant (Ti-Al-V, 0.6-mm-diameter titanium dentine pins; STABILOK) was screwed in. Extra length of the implant was cut at the gingival level.

### PEGASOS Tissue Clearing, Whole-Mount Staining, and 3-D Imaging

PEGASOS tissue clearing was performed following the established protocol (Jing et al. 2019; Yi et al. 2019). Detailed description is provided in the Appendix.

### Statistical Analysis

All experiments were performed 4 times, and representative images were chosen for publication. The number of experiments is provided in each figure or legend. All data are displayed as mean ± SD. GraphPad Prism 7 (GraphPad Software) was used for statistical analysis. Unpaired 2-tailed Student's *t* test was used to compare the difference between 2 independent groups. When more than 2 groups were compared, 1-way analysis of variance (ANOVA) was carried out, followed by Tukey's multiple comparisons test. $P < 0.05$ was considered statistically significant.

## Results

### Gli1$^+$ Cells within the Bone Marrow Space Reside Near Vasculature and Are Largely Negative for Lineage Differentiation Markers

To investigate the distribution and characteristics of Gli1$^+$ cells in adult alveolar bone, *Gli1-Cre$^{ERT2}$;Ai14* mice (GT mice) at 6 wk of age were induced with tamoxifen for 2 d and euthanized on day 5 (Fig. 1A).

The tdTomato$^+$ cells were detected within the bone marrow in the mandibular molar root furcation area (Fig. 1Ba). No tdTomato$^+$ osteocytes were observed. Laminin staining showed that Gli1$^+$ cells within the bone marrow reside around the blood vessels (Fig. 1Bb). GS-IB4 staining further confirmed the association between Gli1$^+$ cells and the vasculature (Fig. 1Bc). Littermates without tamoxifen induction were checked, and no Cre activity was found in the bone marrow area (Appendix Fig. 1A), suggesting the reliability and specificity of the tamoxifen-induced creERT2 line in this study.

Immunostaining of pericyte markers including neuron-glial antigen 2 (NG2) and cluster of differentiation 146 (CD146) showed that most Gli1$^+$ cells were negative for them (Fig. 1Bd, e). The percentages of NG2$^+$/tdTomato$^+$ cells and CD146$^+$/tdTomato$^+$ cells were 18.97% and 29.61%, respectively (Fig. 1C).

The α–smooth muscle actin (αSMA)–positive cells were reported to be a source of periodontal and osteogenic progenitors (Kalajzic et al. 2008; Roguljic et al. 2013). However, as is shown here by immunostaining, αSMA was expressed mainly by arteries within the alveolar bone and more likely to be vascular smooth muscle cells. Gli1$^+$ cells were detected mostly around αSMA$^+$ cells (Fig. 1Bf) and did not largely overlap with αSMA$^+$ cells.

Leptin receptor (LepR) is considered a stem cell marker for long bone (Zhou et al. 2014). In mandibles, LepR$^+$ cells were scarcely detected within the alveolar bone marrow but abundant in soft tissues such as the gingiva, and Gli1$^+$ cells were negative for LepR (Fig. 1Bg).

To study the differentiation status of Gli1$^+$ cells, we performed immunostaining. Periostin is a PDL marker. Gli1$^+$ cells were mostly negative for periostin expression (2.43%) (Fig. 1Bh, C). Sp7 transcription factor (Sp7, also known as Osterix) is a differentiation marker for osteoblasts. Gli1$^+$ cells were mostly negative for Sp7 (8.35%) (Fig. 1Bi, C). Type 1 collagen (Col1) is a secreted protein in bone matrix and is expressed by some fibroblasts within the bone marrow. Gli1$^+$ cells showed almost no expression of Col1 (0.9%) (Fig. 1Bj, C).

### Gli1$^+$ Cells Were Activated and Proliferated Along Blood Vessels after Tooth Extraction

To test the contribution of Gli1$^+$ cells in tooth extraction socket healing, we extracted the mandibular molars and removed PDL in the socket from adult GT mice 3 d after tamoxifen induction.

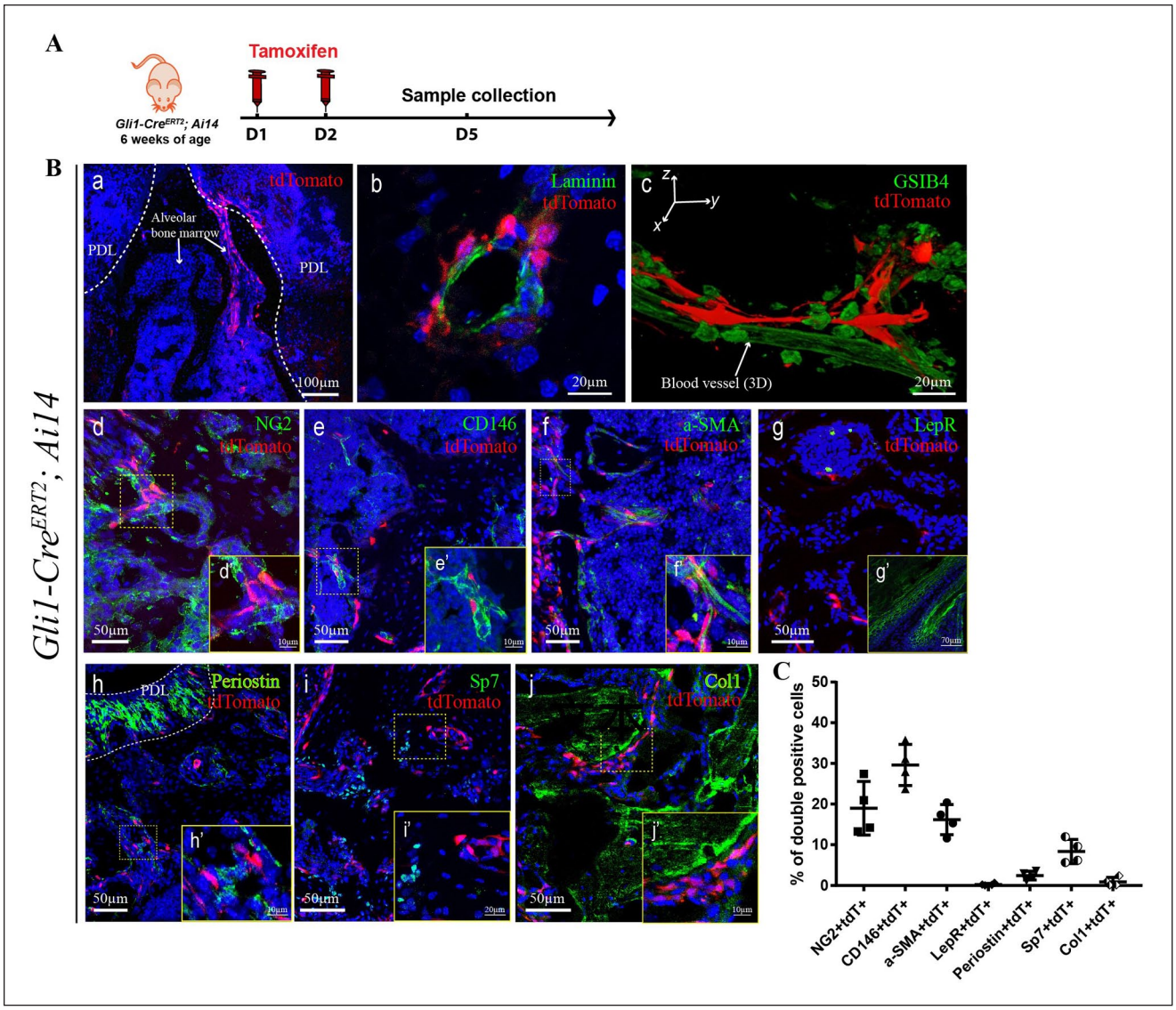


**Figure 1.** Gli1⁺ cells within alveolar bone marrow were surrounding blood vessels and largely negative for pericyte markers and osteogenic lineage markers. (**A**) Experimental timeline. (**B**) The alveolar bones were collected on day 5 after inducton. TdTomato+ cells were visualized in the alveolar bone marrow space (a). Sections at the mandibular first molar furcation of *Gli1-cre*$^{ERT2}$*;Ai14* mice were stained with antibodies against endothelium markers laminin (b) and GS-IB4 (c), pericyte markers NG2 (d) and CD146 (e), stem cell markers α–smooth muscle actin (αSMA) (f) and LepR (g), and lineage markers including periostin (h), Sp7 (i), and type I collagen (j). d′–f′, h′–j′ are enlarged images of boxed areas in d–f, h–j, respectively. g′ is the LepR antibody staining of gingiva on the same section from g, serving as a positive control. (**C**) Percentiles of double-positive cells (i.e., cells that express both tdTomato and specific markers) among tdTomato⁺ cells on sections ($n = 4$).

Mice mandibles were harvested on 1, 7, 14, or 28 d after tooth extraction (Fig. 2A). Middle one-third part of the extraction socket was selected as a region of interest for observing the healing process.

One day after tooth extraction, complete PDL removal was verified histologically (Appendix Fig. 2A). Instead, the socket was filled with a blood clot. No Gli1⁺ cells were detected within the socket. Gli1⁺ cells were observed within the bone marrow adjacent to the socket (Fig. 2Ba, Appendix Fig. 2B). Compared to uninjured conditions, an increased number of Gli1⁺ cells incorporated 5-ethynyl-2′-deoxyuridine (EdU), indicating Gli1⁺ cells were activated into proliferation in response to tooth extraction (Fig. 2Bb, C). Costaining with GS-IB4 indicated that the proliferating Gli1⁺ cells were mostly surrounding the vasculature (Fig. 2Bc).

Seven days after tooth extraction, a large number of tdTomato⁺ cells were visualized within the socket (Fig. 2Da, E). Costaining of laminin antibody indicated the association of these tdTomato⁺ cells with vasculature (Fig. 2Db, F). Sp7 antibody staining showed ~16.8% of Sp7⁺ cells within the socket were also tdTomato⁺, indicating their derivation from Gli1⁺ cells (Fig. 2Dc, G).

Fourteen days after extraction, ~52.81% of cells within the socket were tdTomato⁺ (Fig. 2D d). Laminin antibody staining

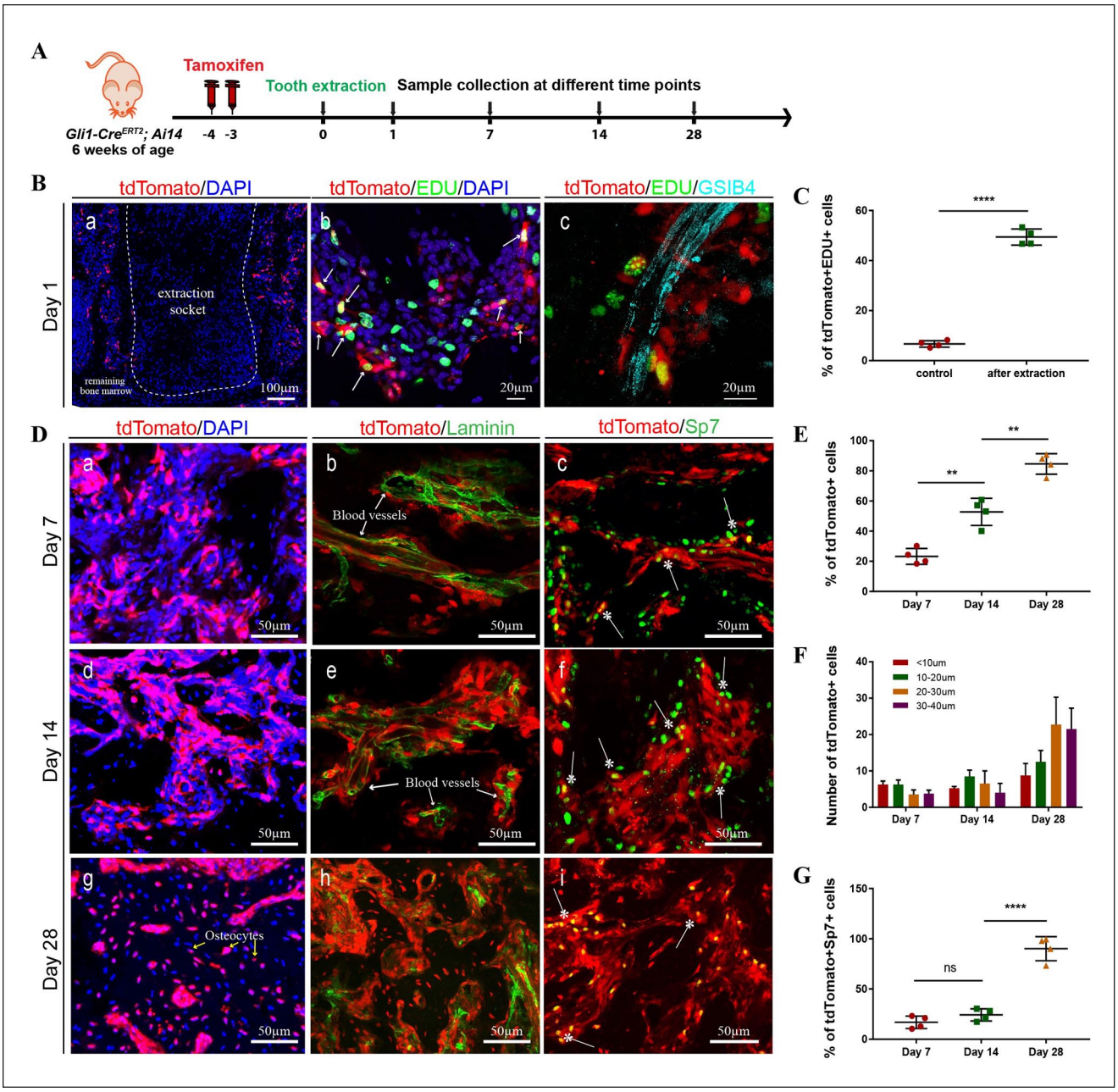


**Figure 2.** Gli1$^+$ cells within alveolar bone marrow were activated after tooth extraction. They migrated along blood vessels and contributed to new bone formation at the extraction site. (**A**) Experimental timeline of tooth extraction and sample collection. (**B**) *Gli1-cre$^{ERT2}$;Ai14* mice extraction site, 1 d after mandibular molar extraction (a). Two-hour EdU incorporation assay showed dividing Gli1$^+$ cells around vasculature 1 day after tooth extraction (b, c). Tamoxifen was injected 5 d prior to the surgery. (**C**) Percentages of tdTomato$^+$/EdU$^+$ cells among tdTomato$^+$ cells within the alveolar bone marrow near socket before and after extraction ($n = 4$). ****$P < 0.0001$. (**D**) Distribution of Gli1$^+$ cells and their derivatives on 7 d (a), 14 d (d), and 28 d (g) after tooth extraction. Immunostaining of laminin (b, e, h) and Sp7 (c, f, i) showed the association of tdTomato$^+$ cells with blood vessels and osteoblasts, respectively. White arrows indicate blood vessels; arrows with star indicate Sp7$^+$/tdTomato$^+$ cells. (**E**) Percentiles of tdTomato$^+$ cells within the extraction socket at different time points ($n = 4$). **$P < 0.01$. (**F**) Number of tdTomato$^+$ cells within each field view at different distances from blood vessels at various time points ($n = 4$). (**G**) Percentiles of Sp7$^+$/tdTomato$^+$ cells among tdTomato$^+$ cells within the extraction socket at different time points ($n = 4$). ****$P < 0.0001$. ns, no significant difference.

indicated tdTomato$^+$ cells were mainly within 20 μm from the vasculature (Fig. 2De, F). Sp7 staining showed ~24% of Sp7$^+$ cells were derived from Gli1$^+$ cells (Fig. 2Df, G).

On day 28 after extraction, ~84% of cells within the socket were tdTomato$^+$ (Fig. 2Dg, E). The tdTomato$^+$ cells were detected at all distances from the vasculature (Fig. 2Dh, F). Over 90% of the Sp7$^+$ cells were tdTomato$^+$, indicating their derivation from Gli1$^+$ cells (Fig. 2Di, G).

LepR$^+$ cells were also known to contribute to extraction socket healing (Zhang, Zhang, et al. 2020). To study the relationship between Gli1$^+$ cells and LepR$^+$ cells, we performed immunostaining with LepR antibody. Seven days after tooth

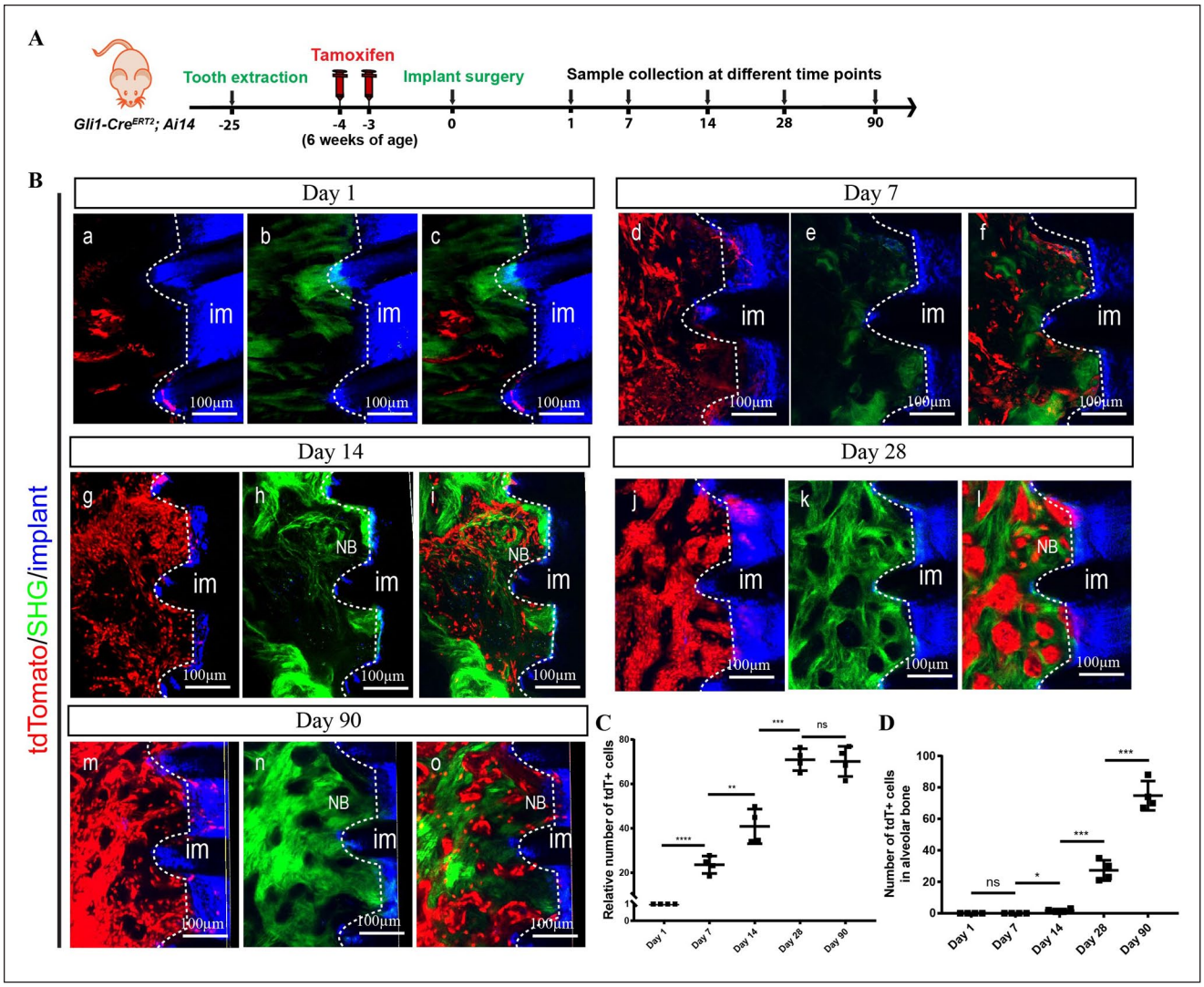


**Figure 3.** Gli1⁺ cells within alveolar bone marrow contributed to the implant osseointegration. (**A**) Experimental timeline of delayed implant placement and sample collection. (**B**) Tissue clearing–based 3-dimensional images of *Gli1-cre$^{ERT2}$;Ai14* mouse mandibles with implants showed contribution of Gli1⁺ cells toward osseointegration on day 1, 7, 14, 28, or 90 after implant placement. Tamoxifen was injected 5 d ahead of implant surgery. (**C**) Normalized tdTomato⁺ cell numbers at different time points were quantified relative to day 1 ($n = 4$). $^{**}P < 0.01$. $^{***}P < 0.001$. $^{****}P < 0.0001$. ns, no significant difference. (**D**) Percentiles of tdTomato⁺ cells among all cells within the alveolar bone marrow at different time points ($n = 4$). $^{*}P < 0.05$. $^{***}P < 0.001$. ns, no significant difference.

extraction, Gli1⁺ cells were negative for LepR (Appendix Fig. 3Aa–c). One month after tooth extraction, most LepR⁺ cells were tdTomato⁺ (Appendix Fig. 3Ae, f), suggesting the derivation of LepR⁺ cells from Gli1⁺ cells.

## *Gli1⁺ Cells in the Alveolar Bone Marrow Contributed to Osseointegration after Delayed Implantation*

Next, we examined contribution of Gli1⁺ cells in the alveolar bone marrow toward implant osseointegration. Adult *Gli1-Cre$^{ERT2}$;Ai14* mice were induced with tamoxifen 3 wk after extraction. A titanium implant was placed in the healed socket 3 d after tamoxifen induction. Mandibles with implants were harvested at various time points afterward (Fig. 3A). After clearing with PEGASOS tissue clearing method, samples were imaged with a 2-photon microscope. Second harmonic generation (SHG) signal was used to show calcified collagen structure of bone tissues (Kim and Bixel 2020), and reflection light was used to outline implants.

One day after placement, remnant bone was observed surrounding the implant in hematoxylin and eosin (H&E)–stained sections (Appendix Fig. 2B). A few tdTomato⁺ cells were detected in the bone marrow adjacent to the implant surface (Fig. 3Ba).

On day 7 after placement, fibrous tissue replaced the bone remnant around the implant (Appendix Fig. 4A, B). The number of tdTomato⁺ cells increased dramatically (Fig. 3Bd–f), which was 20-fold more than that on day 1 (Fig. 3C).

By day 14, the number of tdTomato$^+$ cells continued to increase (Fig. 3Bg, C). As was indicated in both H&E staining and SHG images, fibrous bone also started to form (Fig. 3Bh, Appendix Fig. 4).

By day 28, almost the entire bone marrow space was filled with tdTomato$^+$ cells (Fig. 3Bj, C, Appendix Fig. 5A). Well-organized bone structure was visualized surrounding the implant (Fig. 3Bk, Appendix Figs. 4, 5A). In addition, osteocytes with dendritic processes occupying the bone lacuna (the relatively dark area in SHG imaging) were also tdTomato$^+$ (Appendix Fig. 5B).

By day 90, even more tdTomato$^+$ cells were located within the trabecular bone. Total number of tdTomato$^+$ cells was 70-fold more than that on day 1 (Fig. 3Bm, D). Both micro–computed tomography (CT) and SHG images indicated complete osseointegration surrounding the implant (Fig. 3Bn).

Taken together, the lineage tracing experiments indicated that Gli1$^+$ cells proliferated around the implant and finally differentiated into osteocytes.

## *Gli1$^+$ Cells Are Indispensable for Peri-Implant Bone Formation*

To test if Gli1$^+$ cells are indispensable for bone healing around the implant, we genetically ablated Gli1$^+$ cells using *Gli1-Cre$^{ERT2}$;Ai14;ROSA26$^{eGFP\text{-}DTA}$* (GT-DTA) mice. *Gli1-Cre$^{ERT2}$;Ai14* (GT) mice served as the control group. Surgical procedures on GT and GT-DTA mice were conducted as described above (Appendix Fig. 6A).

Samples were harvested 2 mo after implant placement. Micro-CT results revealed that bone volume around the implants was significantly reduced in the DTA group (Appendix Fig. 6B, C). Deep imaging around implants showed much less tdTomato$^+$ cells in GT-DTA mice compared to GT mice, indicating effective ablation of Gli1$^+$ cells in the GT-DTA mice (cell ablation efficiency: ~84%) (Appendix Fig. 6Da, c). SHG images further showed much less bone surrounding implant in GT-DTA mice (Appendix Fig. 6Db, d). Histological staining of 2-dimensional (2-D) sections showed similar results as 3-D imaging. Well-organized bone structure could be seen in the implant thread grooves in GT mice, while implant thread grooves of GT-DTA mice were filled with fibrous tissues (Appendix Fig. 6E). These findings indicated that the ablation of Gli1$^+$ cells significantly compromised peri-implant bone formation.

## *Gli1$^+$ Cells and Their Derivatives Are Closely Associated with Vasculature during the Implant Osseointegration Process*

To investigate the relationship between Gli1$^+$ cells and vasculature, we generated *Cdh5-Cre$^{ERT2}$;Ai14* mice to label blood vessels (Fig. 4A). Deep imaging showed increased vasculature density near the implant surface from day 1 to day 7 after placement (Fig. 4Ba–d). Enriched vasculature was visualized to directly contact the implant surface on day 28 after surgery (Fig. 4b, e, f). The growth of vasculature was consistent with increased bone density, shown by the SHG signal, near the implant surface (Fig. 4Bb, d, f).

To investigate the association between Gli1$^+$ cells and vasculature, we performed whole-mount staining of GS-IB4. Gli1$^+$ cell and their derivatives were mostly restricted to the perivascular area on day 1 after implant placement (Fig. 4Ca–c, D). On day 7, more Gli1$^+$ cell derivatives were visualized and still close to vasculature (Fig. 4Cd–f, E). On day 28 after placement, tdTomato$^+$ cells had populated the entire peri-implant area but were not restricted to the perivascular area. Nearly half of tdTomato$^+$ cells were near vasculature (<20 μm), while the other half of tdTomato$^+$ cells were in bone tissue far from blood vessels (Fig. 4Cg–i, F).

## *Canonical Wnt Signaling Pathway Played Crucial Roles in Gli1$^+$ Cell-Mediated Implant Osseointegration*

Canonical Wnt signaling is critical in stem cell activation and differentiation (Clevers et al. 2014; Janda et al. 2017; Degirmenci et al. 2018). To study its roles on implant osseointegration, we generated *Gli1-cre$^{ERT2}$;β-catenin$^{flox/flox}$;Ai14* (β-*catenin* inducible conditional knockout, icKO) mice. *Gli1-cre$^{ERT2}$;β-catenin$^{flox/+}$;Ai14* mice served as littermate controls. Tooth extraction was performed at the age of 3 wk for both icKO and littermate control mice. Tamoxifen induction and implant placement were carried out as described above (Fig. 5A).

Micro-CT results indicated that, by day 28, much less bone surrounding implant was detected in the icKO mice compared with the control group (Fig. 5Ba, b, D). On day 90, the bone volume and density reduction surrounding the implant in the icKO group were even more significant (Fig. 5Bc, d, D). Bone–implant contact of the 2 groups showed a similar trend over time (Fig. 5E).

Next, we studied the lineage contribution of Gli1$^+$ cells in the icKO and control groups. One day after implant placement, similar numbers of tdTomato$^+$ cells were detected around the implants in the 2 groups (Fig. 5Ca, b, F). On day 7, less tdTomato$^+$ cells were observed in icKO group, suggesting compromised Gli1$^+$ cell activation in the absence of β-catenin (Fig. 5Cc, d, F). On day 28, while almost all the bone marrow was filled with tdTomato$^+$ cells in the control group, very few tdTomato$^+$ cells were visualized in the icKO group (Fig. 5Ce, f, F). On day 90, the difference in the number of tdTomato$^+$ cells was even more significant between the 2 groups, especially in the trabecular bone (Fig. 5F, G). In addition, in the control group, many tdTomato$^+$ osteocytes were detected within the bone matrix (as indicated by colocalization with the SHG signal). In the icKO group, only very few tdTomato$^+$ osteocytes were observed (Fig. 5Cg, h, F, G), indicating compromised osteocyte differentiation in the icKO group.

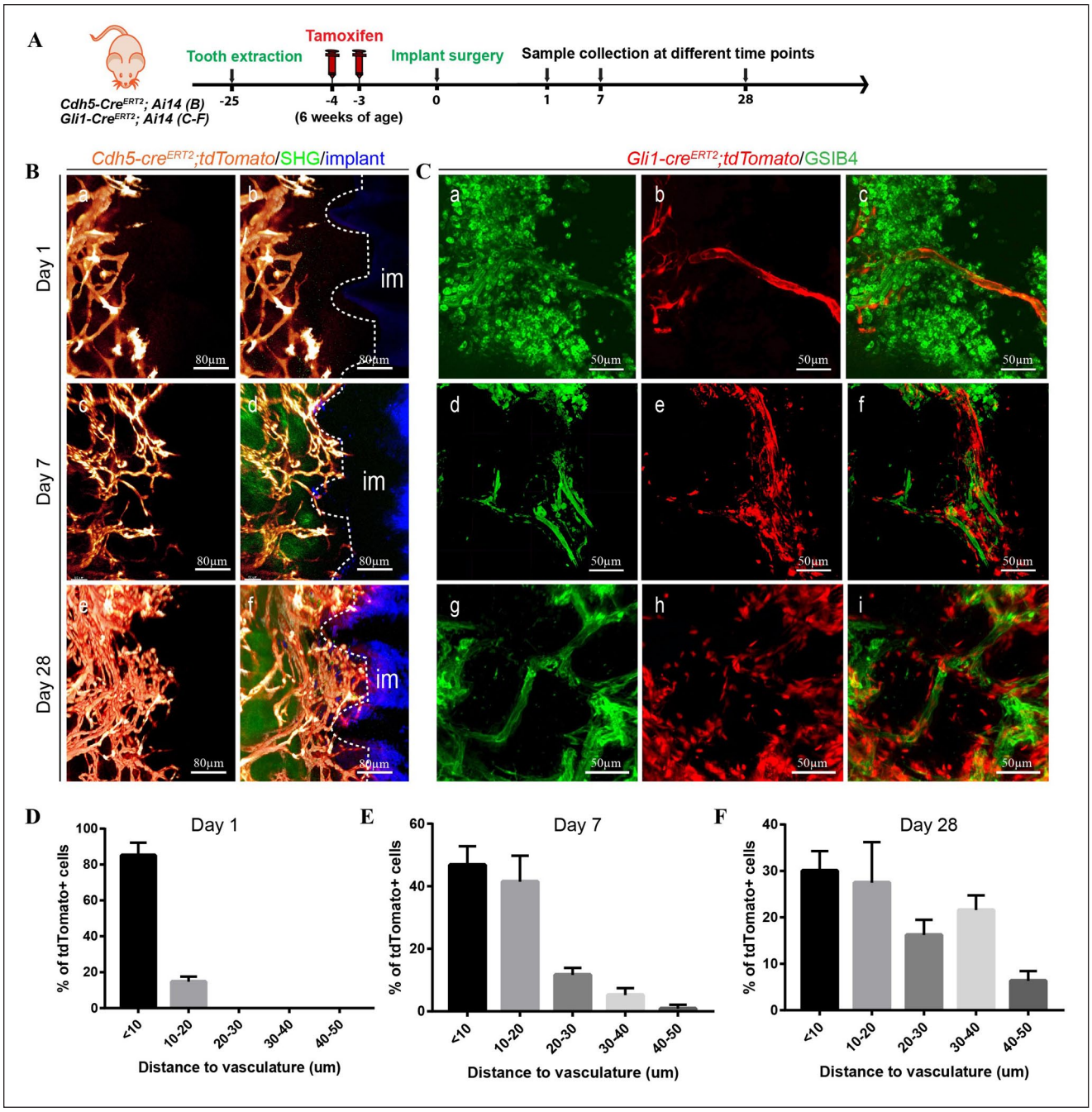


**Figure 4.** Migration of Gli1⁺ cells and their derivatives during osseointegration were closely associated with blood vessels. (**A**) Experimental timeline. (**B**) Tissue clearing–based 3-dimensional images of *Cdh5-cre*$^{ERT2}$*;Ai14* mouse mandibles with implants showed angiogenesis surrounding the titanium implants on day 1, 7, or 28 after implant placement. (**C**) Representative images of *Gli1-cre*$^{ERT2}$*;Ai14* mandibles with implants stained with GS-IB4 showed an association between peri-implant Gli1⁺ cells and vasculature. (**D**–**F**) Percentages of tdTomato⁺ cells at different distances from GS-IB4⁺ blood vessels among all tdTomato⁺ cells on day 1 (D), 7 (E), or 28 (F) after implant placement ($n = 4$).

## Discussion

Implant osseointegration involves bone tissue regeneration surrounding the implant surface. Despite successful clinical application of dental implant, the progenitor cell population driving osseointegration remains an open question. Using lineage tracing and a tissue clearing–based deep imaging technique, we identified Gli1⁺ cells within the alveolar bone marrow as stem cells supporting implant osseointegration. These Gli1⁺ cells surround vasculature and are negative for osteoblast and PDL fibroblast markers. They are activated into proliferation and differentiation to generate new bone and show a close relationship with blood vessels during the whole process. Ablation of Gli1⁺ cells severely compromises

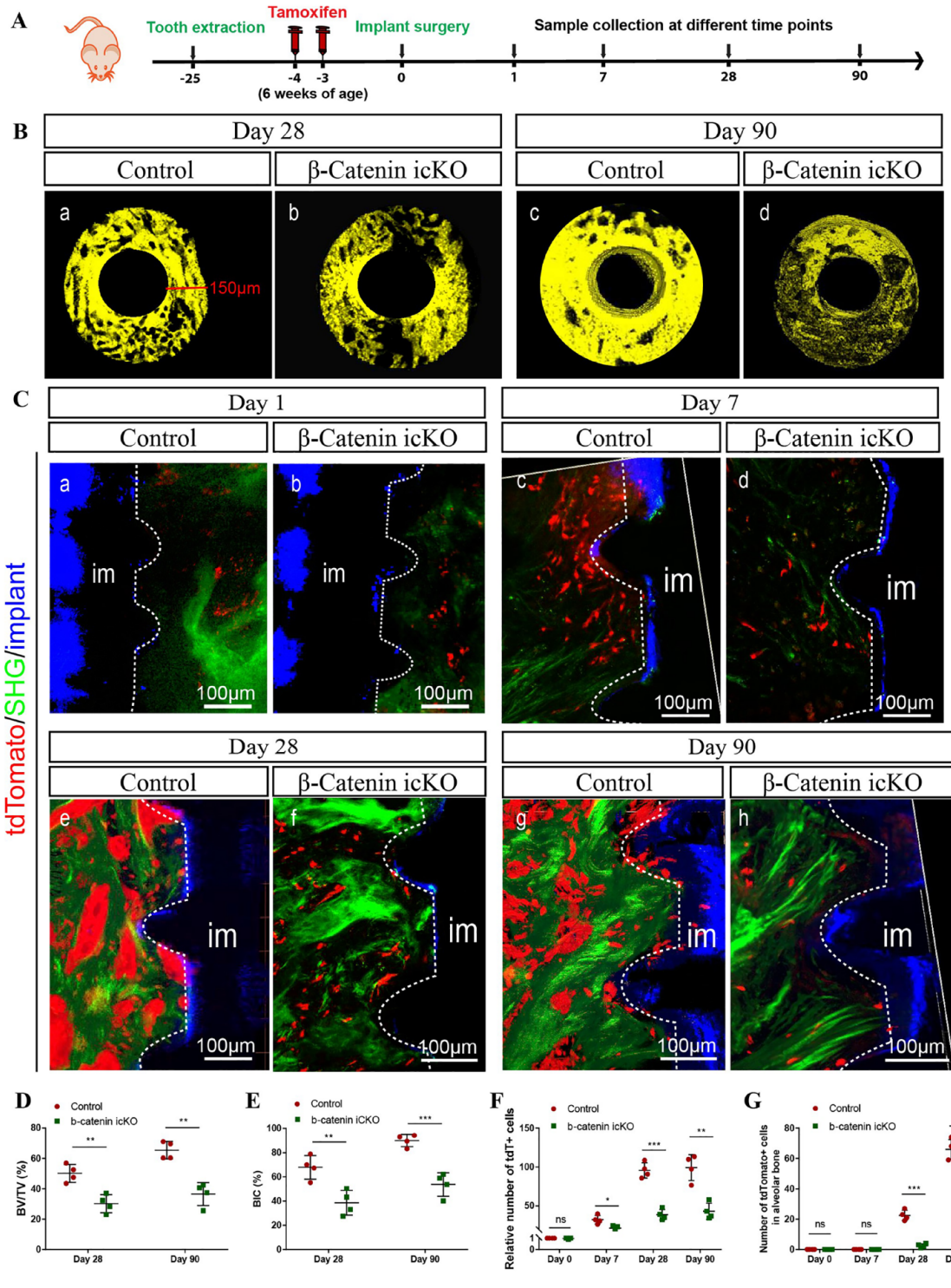


**Figure 5.** Canonical Wnt signaling pathway is required for Gli1$^{+}$ cell-mediated implant osseointegration. (**A**) Experimental timeline. (**B**) Three-dimensional (3-D) reconstruction of micro–computed tomography of *Gli1-cre$^{ERT2}$;Ai14* (control) and *Gli1-cre$^{ERT2}$;β-catenin$^{flox/flox}$;Ai14* (β-*catenin* inducible conditional knockout [icKO]) littermate mice 28 d and 90 d after implant placement. (**C**) Representative 3-D images showed Gli1$^{+}$ cell contribution and new bone formation in control or β-*catenin* icKO group on day 1, 7, 28, or 90 after implant placement. (**D**) Quantitative bone volume fraction analysis of newly formed bone ($n = 4$). $^{**}P < 0.01$. (**E**) Quantitative bone–implant contact (BIC) analysis ($n = 4$). $^{**}P < 0.01$. $^{***}P < 0.001$. (**F**) Normalized tdTomato$^{+}$ cell numbers in control and β-catenin icKO groups at different time points were quantified relative to day 1 ($n = 4$). $^{*}P < 0.05$. $^{**}P < 0.01$. $^{***}P < 0.001$. ns, no significant difference. (**G**) Percentiles of tdTomato$^{+}$ cells in the alveolar bone of control and β-*catenin* icKO sample at different time points ($n = 4$). $^{***}P < 0.001$. ns, no significant difference.

osseointegration. Canonical Wnt signaling pathway is essential for their activation and successful osseointegration. These properties are similar to Gli1$^+$ cells within the PDL (Men et al. 2020). It is possible that Gli1$^+$ cells within the PDL or alveolar bone are the same perivascular stem cell population localized differently.

Both PDL and alveolar bone marrow contain multipotential stem cells (Matsubara et al. 2005; Zhao and Chai 2015; Mashimo et al. 2019). Our previous studies showed that physiologically, PDL Gli1$^+$ cells support turnover of PDL and alveolar bone proper (Men et al. 2020). We speculate Gli1$^+$ cells within bone marrow function to support alveolar trabecular bone turnover under physiological conditions.

Roles of PDL remnant in socket healing remain controversial. Some reported that remnant PDL cells differentiate into osteoblasts for ossification (Devlin and Sloan 2002; Pei et al. 2017). Residual socket *Axin2*$^+$ PDL progenitor may contribute to socket healing (Yuan, Pei, Zhao, Tulu, et al. 2018). However, this study could not exclude the possible contribution of progenitor cells outside the socket because *Axin2* was also widely expressed by osteoblasts lining the alveolar bone marrow. On the other hand, there are also studies showing that the amount of newly formed bone was not significantly affected by excavating PDL residual after tooth extraction (Isaka et al. 2001). In the clinic, socket healing can still occur in periodontitis patients with severe PDL tissue loss. Our study does not exclude the roles of residual PDL on socket healing. Instead, we showed that alveolar bone marrow Gli1$^+$ cells made a significant contribution.

LepR$^+$ cells within the alveolar bone marrow were shown to be stem cells essential for tooth extraction socket healing (Zhang, Zhang, et al. 2020). Our results from immunostaining of LepR suggests that LepR$^+$ cells might be derived from Gli1$^+$ cells and could be a subpopulation. This is similar to the LepR$^+$ cells in the PDL tissue (Men et al. 2020). Further studies are needed to verify the relationship between these 2 populations.

Canonical Wnt signaling pathway is critical for regulating stem cell proliferation and fate determination (Clevers et al. 2014; Janda et al. 2017; Degirmenci et al. 2018). Our inducible conditional knockout experiments indicated that the canonical Wnt signaling pathway is indispensable for activation of Gli1$^+$ cells and implant osseointegration. This is consistent with a previous study based on *Axin2*$^+$ PDL progenitor cells (Yuan, Pei, Zhao, Tulu, et al. 2018).

Implant–tissue interface is the key issue for implant studies. Our current work showed that tissue clearing–based deep imaging can be a powerful tool. Tissues surrounding the implant were turned transparent with well-preserved fluorescent signal and interface morphology. Compared with micro-CT, deep imaging can be multicolor and achieve much higher resolution.

In conclusion, we identified Gli1$^+$ cells within alveolar bone marrow as a stem cell source for tooth extraction socket healing and delayed dental implant osseointegration. Canonical Wnt signaling pathway regulates stem cell activation. Our study will help to better understand the mechanism of implant osseointegration.

## Author Contributions

Y. Yi, H. Zhao, contributed to conception, design, data acquisition, analysis, and interpretation, drafted and critically revised the manuscript; W. Stenberg, W. Luo, contributed to data interpretation, critically revised the manuscript; J.Q. Feng, contributed to data analysis, critically revised the manuscript. All authors gave final approval and agree to be accountable for all aspects of the work.

## Declaration of Conflicting Interests

The authors declared no potential conflicts of interest with respect to the research, authorship, and/or publication of this article.

## Funding

The authors disclosed receipt of the following financial support for the research, authorship, and/or publication of this article: This study was supported by startup funding from the Texas A&M University to H. Zhao and R01 DE028291 grant from the National Institutes of Health (NIH)/National Institute of Dental and Craniofacial Research (NIDCR) to J.Q. Feng.

## References

Branemark PI, Adell R, Breine U, Hansson BO, Lindstrom J, Ohlsson A. 1969. Intra-osseous anchorage of dental prostheses. I. Experimental studies. Scand J Plast Reconstr Surg. 3(2):81–100.

Buser D, Sennerby L, De Bruyn H. 2017. Modern implant dentistry based on osseointegration: 50 years of progress, current trends and open questions. Periodontol 2000. 73(1):7–21.

Calvo-Guirado JL, Ortiz-Ruiz AJ, Negri B, Lopez-Mari L, Rodriguez-Barba C, Schlottig F. 2010. Histological and histomorphometric evaluation of immediate implant placement on a dog model with a new implant surface treatment. Clin Oral Implants Res. 21(3):308–315.

Canellas JVDS, Medeiros PJD, Figueredo CMDS, Fischer RG, Ritto FG. 2019. Which is the best choice after tooth extraction, immediate implant placement or delayed placement with alveolar ridge preservation? A systematic review and meta-analysis. J Craniomaxillofac Surg. 47(11):1793–1802.

Chappuis V, Engel O, Reyes M, Shahim K, Nolte LP, Buser D. 2013. Ridge alterations post-extraction in the esthetic zone: a 3D analysis with CBCT. J Dent Res. 92(12 Suppl):195S–201S.

Clevers H, Loh KM, Nusse R. 2014. Stem cell signaling. An integral program for tissue renewal and regeneration: Wnt signaling and stem cell control. Science. 346(6205):1248012.

Degirmenci B, Valenta T, Dimitrieva S, Hausmann G, Basler K. 2018. Gli1-expressing mesenchymal cells form the essential Wnt-secreting niche for colon stem cells. Nature. 558(7710):449–453.

Devlin H, Sloan P. 2002. Early bone healing events in the human extraction socket. Int J Oral Maxillofac Surg. 31(6):641–645.

Eilken HM, Diéguez-Hurtado R, Schmidt I, Nakayama M, Jeong H-W, Arf H, Adams S, Ferrara N, Adams RH. 2017. Pericytes regulate VEGF-induced endothelial sprouting through VEGFR1. Nat Commun. 8(1):1574.

He T, Cao C, Xu Z, Li G, Cao H, Liu X, Zhang C, Dong Y. 2017. A comparison of micro-CT and histomorphometry for evaluation of osseointegration of PEO-coated titanium implants in a rat model. Sci Rep. 7(1):16270.

Isaka J, Ohazama A, Kobayashi M, Nagashima C, Takiguchi T, Kawasaki H, Tachikawa T, Hasegawa K. 2001. Participation of periodontal ligament cells with regeneration of alveolar bone. J Periodontol. 72(3):314–323.

Janda CY, Dang LT, You C, Chang J, de Lau W, Zhong ZA, Yan KS, Marecic O, Siepe D, Li X, et al. 2017. Surrogate Wnt agonists that phenocopy canonical Wnt and β-catenin signalling. Nature. 545(7653):234–237.

Jing D, Yi Y, Luo W, Zhang S, Yuan Q, Wang J, Lachika E, Zhao Z, Zhao H. 2019. Tissue clearing and its application to bone and dental tissues. J Dent Res. 98(6):621–631.

Jing D, Zhang S, Luo W, Gao X, Men Y, Ma C, Liu X, Yi Y, Bugde A, Zhou BO, et al. 2018. Tissue clearing of both hard and soft tissue organs with the PEGASOS method. Cell Res. 28(8):803–818.

Kalajzic Z, Li H, Wang LP, Jiang X, Lamothe K, Adams DJ, Aguila HL, Rowe DW, Kalajzic I. 2008. Use of an alpha-smooth muscle actin GFP reporter to identify an osteoprogenitor population. Bone. 43(3):501–510.

Kim J, Bixel MG. 2020. Intravital multiphoton imaging of the bone and bone marrow environment. Cytometry A. 97(5):496–503.

Mashimo T, Sato Y, Akita D, Toriumi T, Namaki S, Matsuzaki Y, Yonehara Y, Honda M. 2019. Bone marrow–derived mesenchymal stem cells enhance bone marrow regeneration in dental extraction sockets. J Oral Sci. 61(2):284–293.

Matsubara T, Suardita K, Ishii M, Sugiyama M, Igarashi A, Oda R, Nishimura M, Saito M, Nakagawa K, Yamanaka K, et al. 2005. Alveolar bone marrow as a cell source for regenerative medicine: differences between alveolar and iliac bone marrow stromal cells. J Bone Miner Res. 20(3):399–409.

Men Y, Wang Y, Yi Y, Jing D, Luo W, Shen B, Stenberg W, Chai Y, Ge W-P, Feng JQ, et al. 2020. Gli1$^+$ periodontium stem cells are regulated by osteocytes and occlusal force. Dev Cell. 54(5):639–654.e6.

Pei X, Wang L, Chen C, Yuan X, Wan Q, Helms JA. 2017. Contribution of the PDL to osteotomy repair and implant osseointegration. J Dent Res. 96(8):909–916.

Roguljic H, Matthews BG, Yang W, Cvija H, Mina M, Kalajzic I. 2013. In vivo identification of periodontal progenitor cells. J Dent Res. 92(8):709–715.

Schneider RK, Mullally A, Dugourd A, Peisker F, Hoogenboezem R, Van Strien PMH, Bindels EM, Heckl D, Büsche G, Fleck D, et al. 2017. Gli1$^+$ mesenchymal stromal cells are a key driver of bone marrow fibrosis and an important cellular therapeutic target. Cell Stem Cell. 20(6):785–800.e8.

Sena IFG, Prazeres P, Santos GSP, Borges IT, Azevedo PO, Andreotti JP, Almeida VM, Paiva AE, Guerra DAP, Lousado L, et al. 2017. Identity of Gli1$^+$ cells in the bone marrow. Exp Hematol. 54:12–16.

Shi Y, He G, Lee WC, McKenzie JA, Silva MJ, Long F. 2017. Gli1 identifies osteogenic progenitors for bone formation and fracture repair. Nat Commun. 8(1):2043.

Tainaka K, Kuno A, Kubota SI, Murakami T, Ueda HR. 2016. Chemical principles in tissue clearing and staining protocols for whole-body cell profiling. Annu Rev Cell Dev Biol. 32:713–741.

Tuan RS. 2011. Role of adult stem/progenitor cells in osseointegration and implant loosening. Int J Oral Maxillofac Implants. 26(Suppl):50–62.

Yi Y, Men Y, Jing D, Luo W, Zhang S, Feng JQ, Liu J, Ge WP, Wang J, Zhao H. 2019. 3-Dimensional visualization of implant-tissue interface with the polyethylene glycol associated solvent system tissue clearing method. Cell Prolif. 52(3):e12578.

Yuan X, Pei X, Zhao Y, Li Z, Chen CH, Tulu US, Liu B, Van Brunt LA, Brunski JB, Helms JA. 2018. Biomechanics of immediate postextraction implant osseointegration. J Dent Res. 97(9):987–994.

Yuan X, Pei X, Zhao Y, Tulu US, Liu B, Helms JA. 2018. A Wnt-responsive PDL population effectuates extraction socket healing. J Dent Res. 97(7):803–809.

Zhang D, Zhang S, Wang J, Li Q, Xue H, Sheng R, Xiong Q, Qi X, Wen J, Fan Y, et al. 2020. LepR-expressing stem cells are essential for alveolar bone regeneration. J Dent Res. 99(11):1279–1286.

Zhang G, Li Q, Yuan Q, Zhang S. 2020. Spatial distributions, characteristics, and applications of craniofacial stem cells. Stem Cells Int. 2020:8868593.

Zhao H, Chai Y. 2015. Stem cells in teeth and craniofacial bones. J Dent Res. 94(11):1495–1501.

Zhao H, Feng J, Ho TV, Grimes W, Urata M, Chai Y. 2015. The suture provides a niche for mesenchymal stem cells of craniofacial bones. Nat Cell Biol. 17(4):386–396.

Zhao H, Feng J, Seidel K, Shi S, Klein O, Sharpe P, Chai Y. 2014. Secretion of Shh by a neurovascular bundle niche supports mesenchymal stem cell homeostasis in the adult mouse incisor. Cell Stem Cell. 14(2):160–173.

Zhou BO, Yue R, Murphy MM, Peyer JG, Morrison SJ. 2014. Leptin-receptor-expressing mesenchymal stromal cells represent the main source of bone formed by adult bone marrow. Cell Stem Cell. 15(2):154–168.